Uncertainty in Nowcasting of Radar Rainfall

a case study of the GLUE methodology

Thorndahl, Søren Liedtke; Rasmussen, Michael R.; Nielsen, Jesper Ellerbæk; Larsen, Jakob Badsberg

Published in:
Advances in Radar Technology

Publication date:
2010

Document Version
Publisher's PDF, also known as Version of record

Uncertainty in nowcasting of radar rainfall - a case study of the GLUE methodology

Thorndahl, S.[1], Rasmussen, M.R.[1], Nielsen, J.E.[1], Larsen, J.B.[1]

[1]Aalborg University, Department of Civil Engineering,

Sohngaardsholmsvej 57, 9000 Aalborg, Denmark, *st@civil.aau.dk*

Søren Thorndahl

1. Introduction

Weather radar based nowcasting (or short term forecasting) of rainfall in urban areas is an evolving topic as it is an economically feasible solution handle some of the challenges of climate changes. The perspectives within hydrological and urban hydrological modelleing are many. In urban drainage, there is a large potential to predict rain with a certain lead time, in order to implement real time operations of urban drainage systems to facilitate storage of rain water in some parts of the drainage system in order to prevent flooding or overflow to receiving waters elsewhere. Another feasible potential is activation of warning systems of urban flooding based on rainfall nowcasting in combination with a real time urban drainage model. In the end, these solutions are ways of reducing construction or reconstructions costs of drainage systems in the changing climate. During the past few years the applications have evolved from development of methods and case studies to actual real time operation based on nowcasting, e.g. Aspegren (2001), Einfalt et al. (2004), Achleitner et al. (2009), Schellart et al. (2009) and Thorndahl et al. (2009, 2010). However, in excitement of the current development in technology, the uncertainty of rainfall nowcasting is often ignored in operation applications, and thus the risk of making wrong decisions based on defective nowcasts is impending. The uncertainty quantification is further complicated by the fact that prediction of urban rainfall requires small time scales as the runoff response is fast. Therefore, it is not sufficient to predict correct rainfall volumes, but the rain intensities have to be precise in order to apply nowcasting in urban areas.

Uncertainties related to quantitative precipitation estimates from weather radars have been investigated by several authors, e.g. Borga (2002), Villarini et al. (2008) and Villarini and Krajewski (2010); and Grecu and Krajewski (2000) and Fabry and Seed (2009) investigated uncertainty related to quantitative precipitation forecasting using radars, however on a larger temporal scale than required within the area of urban hydrology. Therefore, this study will investigate the uncertainties related to nowcasting of weather radar based rainfall on a small spatial and temporal scale by implementation of a stochastic shell on top of the existing model framework (Thorndahl et al. 2009 and Thorndahl and Rasmussen 2009).

The model is based on extrapolation of radar images and has its origin in the TREC and CO-TREC models (Rinehart and Garvey 1978; Mechlenburg 2000; Li et al. 1995). This is combined with the Monte Carlo based Generalized Likelihood Uncertainty Estimation (GLUE) method (Beven and Binley 1992) in which the nowcast model is conditioned on observations in order to evaluate uncertainties. GLUE has been applied within a wide range of hydrological applications and urban hydrological applications (e.g. Thorndahl et al. 2008), but as far as the authors know never in the context of nowcasting and extrapolation of radar rainfall.

Besides evaluating the nowcast model as a function of the lead time and investigating the sensitivity of model parameters, it is examined, if the concept can be applied for predicting rain intensities with confidence bounds linked to each point in space and time as well as predicting probability of rain occurrence in a specific area. The main purpose is to gain knowledge on the limitations and constraints of the model during different meteorological conditions and to obtain realistic values and posterior distributions of parameters in order to, on the longer term, be able to calculate uncertainty estimates in real time nowcasting.

2. Nowcast model

The short term forecast algorithm applied in this study is developed at Aalborg University and is based on the TREC-algorithm (TRacking of Echoes with Correlation, Rinehart and Garvey 1978) and the CO-TREC (Continuous-TREC, Mechlenburg 2000; Li et al. 1995). Furthermore, Van Horne (2002) has inspired some of the spatial smoothing algorithms which are implemented in the model.

In the first step of the model (*Preprocessing*), the radar data is spatially averaged over a number of *time steps* (*N*) and filtered over the *filter grid size* (*fgz*). Moreover, a *reflectivity cutoff* value is implemented (Z_{min}) in order to reduce noise produced by low reflectivity. In the second step (*Correlation Analysis*), a 2D cross-correlation analysis is applied on subset boxes of the radar image (*Box size: B*). These boxes are displaced in pairs by the *displacement distance* (d_B) and the correlation coefficient is calculated for all possible pairs of boxes. The *search area* (A_{max}) defines the area in which to find the box pairs with the highest correlation. In order for the correlation coefficient to be calculated a *minimum percentage* (r_{min}) of the pixels in the individual boxes must contain values (rainfall). In the end the correlation analysis leads to a number of translation vectors (cf. the *TREC* algorithm) corresponding to the movement of the rain. The translation vectors are interpolated into a number of squares (*Square size: S*). In order to avoid defective or unrealistic advection, the field of vectors is smoothed by implementation of a moving average between the radar images over time and some constraints on the variations of speeds and directions (*CO-TREC*). These constraints involve four parameters: the maximum ratio between the global translation vector velocity and the individual velocities in each square ($V_{max,global}$); the maximum ratio between the velocities in two successive squares ($V_{max,local}$); the maximum difference between the angle of the global vector and the individual vectors in the squares ($a_{max,global}$); and finally the maximum difference between the angles of two successive squares ($a_{max,local}$). An example of the vector field (squares) in TREC and CO-TREC is shown in fig. 1. In the final step of the nowcast model (*Extrapolation*) the latest calibrated radar image is extrapolated a number of time steps into the future based on the field of smoothened vectors. The vectors in the different time steps are independent. The parameters included in the model are presented in table 1.

Prior to the nowcast model, the radar data reflectivity is converted into rain intensities using a standard Marshall-Palmer conversion (Marshall and Palmer 1948). This process might also be randomized, but this would however remove the focus from nowcast model in the present paper and is therefore omitted.

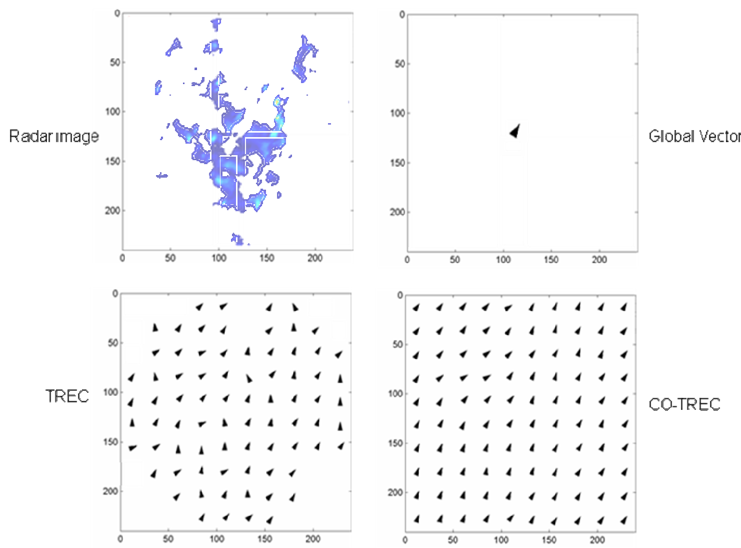

Fig. 1. Example of vectors in TREC and CO-TREC.

The model is implemented in a MATLAB environment, and is currently running on-line with eight different X- and C-band radars as presented in Thorndahl et al. (2009).

The nowcast model is validated using three different parameters: The 2D correlation coefficient (R^2) for a masked area of the radar image (see section 4), and the *critical success index* (*CSI*, Li et al. 1995). CSI is a measure of the model's ability to predict rain in the correct pixels and does not take the intensity levels into account. Ranging from zero to one, both correlation measures are used to estimate the maximum effective lead time of the nowcast model.

3. Stochastic model

The concept of the generalized likelihood uncertainty estimation (GLUE) method (Beven and Binley 1992) is to execute a large number of Monte Carlo simulations with random parameter sets selected from prior probability distribution functions for each parameter. For each model simulation a likelihood measure is calculated in order to reflect the goodness of fit in comparison with some observation dataset. Simulations that are not considered to be acceptable are rejected as non-behavioural (given a likelihood of zero). From the remaining set of behavioural simulations, it is possible to derive posterior probability density functions for both parameters and predictions using the likelihood measure as a weighting factor. The intention is to allow for the demonstrated possibility that many different models and parameter sets might provide acceptable predictions when compared with the available observations, the equifinality thesis (Beven, 2006). GLUE differs from traditional Bayesian methods as the likelihood measure is defined empirically. In the present paper the likelihood is defined as the arithmetic mean of the validation parameter (either R^2 or CSI) over the total lead time. These likelihood measures will ensure a measure of the overall fit of the nowcast model. The likelihood based on R^2 is applied when rain intensities are estimated and the likelihood based on the CSI index is applied when binarily occurrence of rain is considered.

The randomized parameters are presented in table 1 along with the prior probability distributions of each parameter (uniform distributions).

Table. 1. Continuity of the nowcast model, parameters and prior distributions.

Model Step	Parameter	Symbol	Distribution	Type
1) Preprocessing	Number of time steps for averaging (-)	N	U(2,7)	Integer
	Filter grid size (pixels)	fgz	U(1,240)	Integer
	Reflectivity cut-off (dBz)	Z_{min}	U(0,350)	Real
2) Correlation analysis	Correlation box size (pixels)	B	U(1,60)	Integer
	Box displacement (pixels)	dB	U(1,120)	Integer
	Search area (pixels)	A_{max}	U(1,15)	Integer
	Minimum percentage of rain in box (%)	r_{min}	U(0,1)	Real
	Square size (interpolated boxsize) (pixels)	S	U(6,120)	Integer
3) Smoothing	Max. ratio between global vector velocity and individual velocities (-)	$V_{max, global}$	U(0,5)	Real
	Max. ratio between velocities in two successive squares (-)	$V_{max, local}$	U(0,5)	Real
	Max. difference between angle of the global vector and individual vectors (rad)	$\alpha_{max,global}$	U(0, π)	Real
	Max. difference between angles of two successive squares (rad)	$\alpha_{max,local}$	U(0, π)	Real
4) Extrapolation				

4. Data and model setup

The data applied in this study is from the C-band weather radar located in Sindal in the northern part of Denmark. The radar is owned and operated by Danish Meteorological Institute (DMI, Gill et al. 2006). The radar has a range of 240 km with a temporal resolution of 10 min. The data is an extraction of the lowest cappi layer with a Cartesian grid of 2 x 2 km pixels. DMI recommends quantitative precipitation estimates in the range of 0 to 75-100 km. Therefore, the radar image is masked to the 100 km radius, calculating R^2. The total lead time of the nowcast model is fixed to 120 min.

The model is evaluated using GLUE during three different conditions: (1) a stratiform front moving from SW (Fig. 2), (2) a cyclonic low pressure rotation (Fig. 3), and (3) scattered convective storms (Fig. 4). For each of the three events 10,000 Monte Carlo simulations are completed.

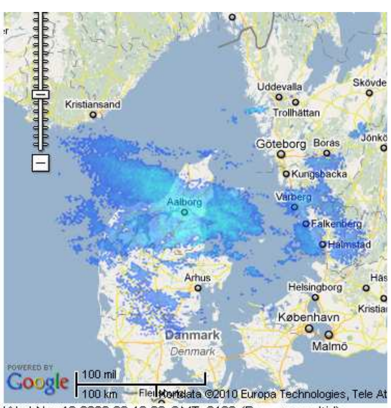

FIG. 2. Event 1, Stratiform event (Google Maps).

FIG. 3. Event 2, Cyclonic rotation event (Google Maps).

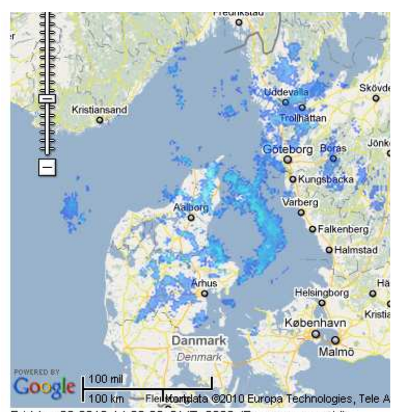

FIG. 4. Event 3, Convective event (Google Maps).

5. Results

In this section selected plots are presented in order to describe the model performance during the three different conditions. In order to sort out the simulations with the worst goodness of fit simulations with a likelihood lower than 0.3 are rejected. Fig. 7 shows the so-called dotty plots in which the calculated likelihoods are shown as a function of the parameter values for each parameter. It is obvious that many of the subplots has equal likelihood as a function of the parameter value (flat tops), indicating either low sensitivity or that the parameters are heavily correlated. Studying the posterior distributions show that the latter is not the case. Some of the parameters have a clear optimum, e.g. the *Search Area* (A_{max}) and the *reflectivity cutoff* (Z_{min}). Comparing the dotty plots of the two other events (not shown but summarized in Tab. 2), it is obvious that *event 1* has the highest likelihood values and the most accepted simulations. This result is as expected as the stratiform rain has a rather uniform and straight movement. The likelihood values for the cyclonic rotation (*event 2*) and the convective storms (*event 3*) varies more than in the two other events, indicating that the parameters are more sensitive during these meteorological conditions.

Fig. 5 and 6 show the masked correlation coefficient (R^2) and the critical success index as a function of the lead time for *event 2*. R^2, representing the intensity levels, drops quite fast whereas CSI, representing the displacement of the rain is above 0.5 until a mean lead time of approx. 60 min. There is quite a large dispersion around the mean values of the performance parameters which is a result of relatively low acceptance threshold. If the threshold was assigned a higher value the mean values would be larger and the dispersion smaller.

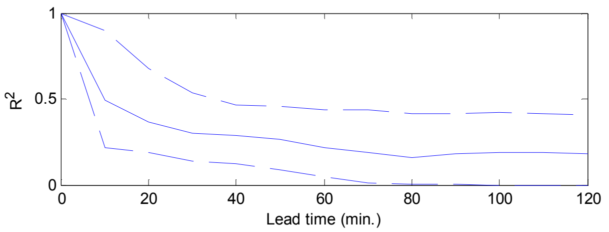

FIG. 5. R^2 as a function of the lead time with 5 and 95 % prediction bands (event 2)

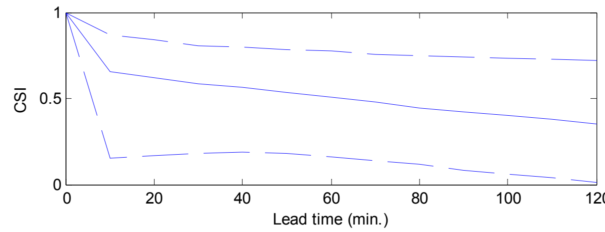

FIG. 6. CSI as a function of the lead time with 5 and 95 % prediction bands (event 2)

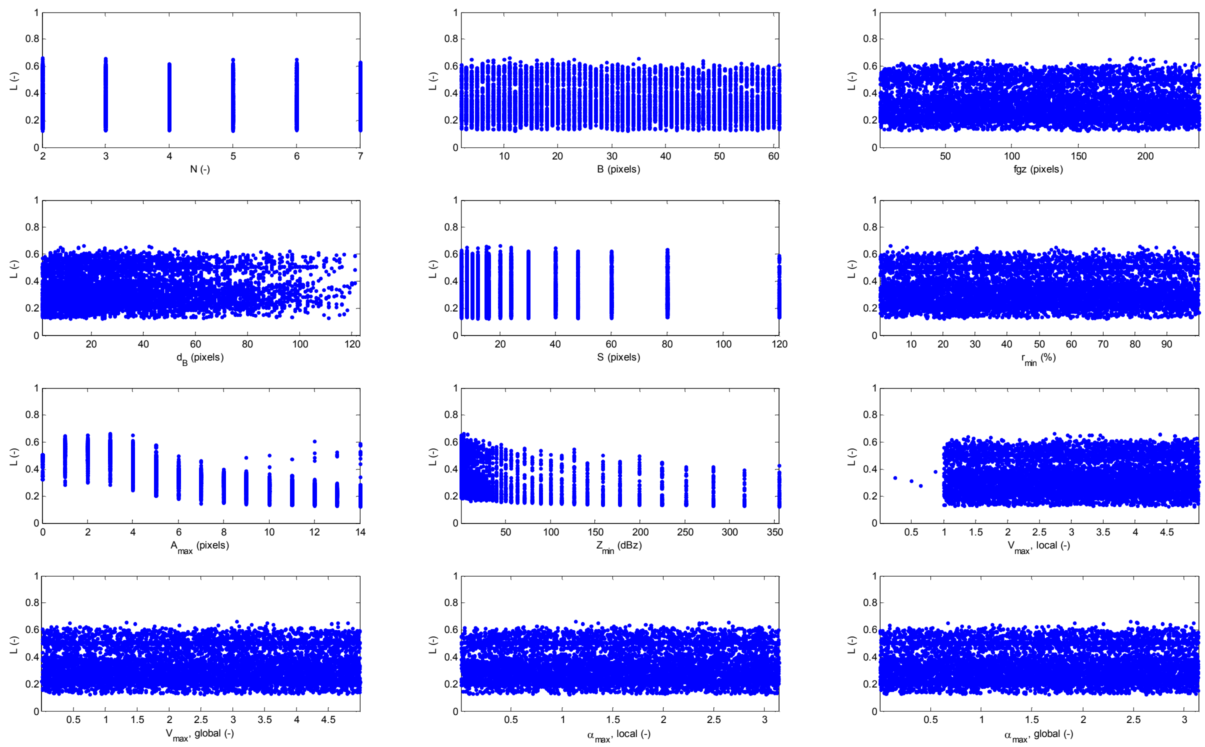

FIG. 7. Likelihoods (based on R^2) as a function of parameter values – event 1.

Table 2. Number of accepted simulations and mean and standards deviations of the likelihood values.

	Likelihood based on R^2			Likelihood based on CSI		
	Accepted	Mean (L)	Standard dev. (L)	Accepted	Mean (L)	Standard dev. (L)
Event 1	6653	0.46	0.12	7069	0.65	0.17
Event 2	2725	0.37	0.06	6267	0.42	0.07
Event 3	1064	0.35	0.04	3204	0.34	0.03

Fig. 10, 11, and 12 show the probability of rain (scaled likelihood based on CSI) at four different lead times for the three events. Obviously, the largest probabilities occur at the smallest lead times. Furthermore, the largest probabilities are observed in event 1 as this type rain is the simplest to predict.

Figure 8 and 9 show an example of predicted rain intensities in two pixels for *event 1* and *3*. The first event shows some divergence between the predicted mean value and the observed; however the observed values are within the predicted 5 and 95 % prediction bands, indicating that the predicted range is correct.

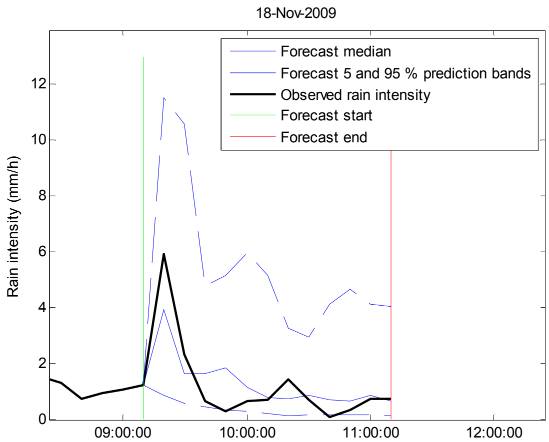

FIG. 8. Time series of observed and forecasted rain, Event .1

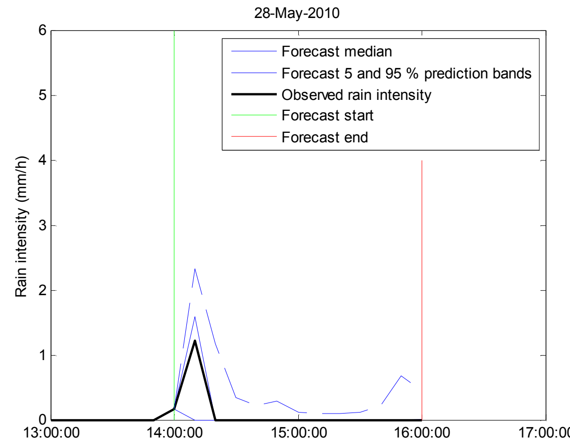

FIG. 9. Time series of observed and forecasted rain, Event 3

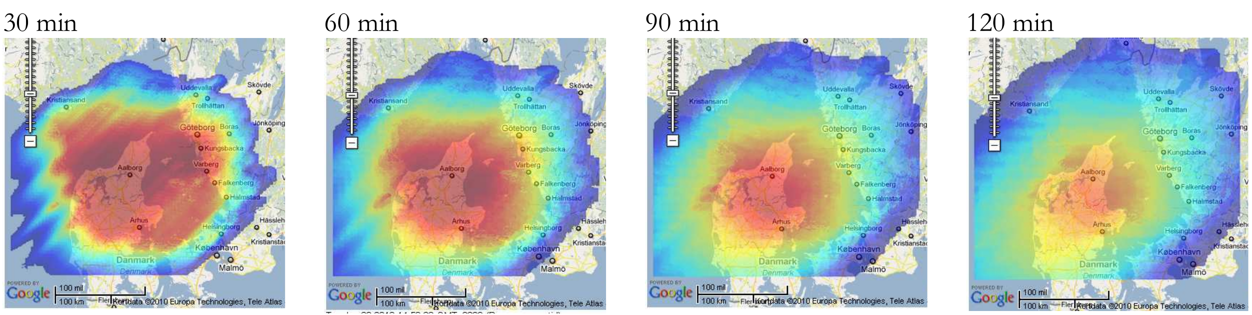

FIG. 10. Probability of rain occurrence, cf. a rain intensity larger than 0. Deep red corresponds to a probability of 1 and dark blue to a probability of 0, event 1(Google maps).

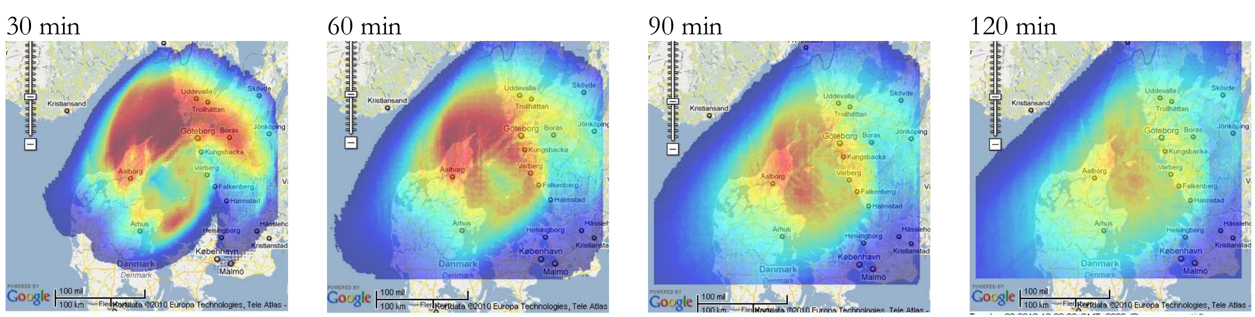

FIG. 11. Probability of rain occurrence, cf. a rain intensity larger than 0. Deep red corresponds to a probability of 1 and dark blue to a probability of 0, event 2(Google maps).

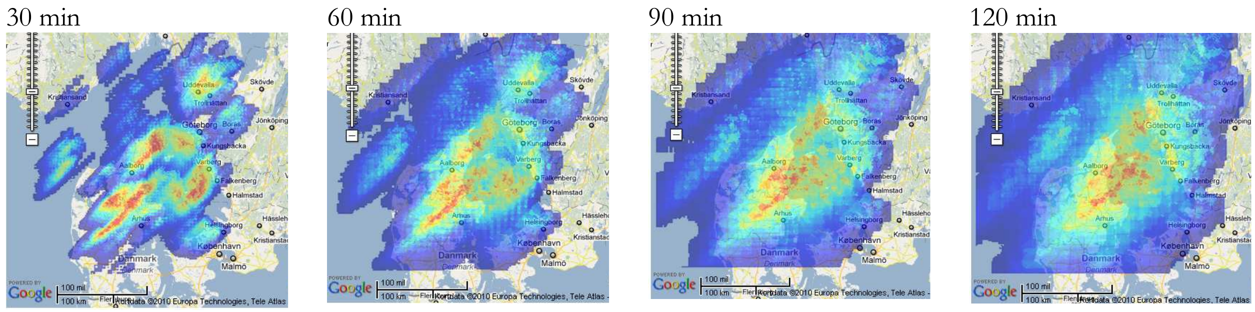

FIG. 12. Probability of rain occurrence, cf. a rain intensity larger than 0. Deep red corresponds to a probability of 1 and dark blue to a probability of 0, event 3(Google maps).

5. Discussion

Through this analysis satisfying results are obtained with regards to the overall nowcast model performance, and in general it is possible to a quite reliable nowcast within 100 km radius of the radar with a lead time of 60 minutes. Beyond 60 minutes and outside the 100 km range it is only possible to predict non-quantitative precipitation. The best model performance is found during stratiform conditions (*event 1*) due to the semi steady state conditions. The cyclonic rotation (*event 2*) is also modeled with satisfying results, however with lower likelihoods than the former. The convective storms (*event 3*) are more difficult to forecast due to more transient meteorological conditions. Furthermore, the model fails in event 3 as the nowcast is only based on extrapolation of the radar images and development of the rain is not included. Increase or decrease in rain intensity in convective cells is therefore not modeled. Currently, the authors are developing a new version of the nowcast model which includes a synthetic particle tracking module for simulation of the dynamics of the rain.

The concept of GLUE has shown to be very applicable in terms of testing model and model parameter sensitivity as well as estimating the uncertainties of predicted rain intensities.

The fact that the model show very little sensitivity, and therefore low variability in the posterior distributions, with regards to some of the parameter are rather unexpected, however application of different likelihood measures might entail larger variations. Furthermore, if the likelihoods are calculated locally, e.g. corresponding to a specific area of focus, instead of globally more deviations from the uniform prior distributions is expected. This will be the object of another paper.

As written in the introduction, the object of this paper is obviously to be able to do uncertainty estimates applying the nowcast model in real time based on the posterior distributions from this analysis and a simple stochastic sampling method, e.g. crude Monte Carlo simulations. However, in order to derive reliable posterior distributions for implementation in real time applications, a more thorough review of likelihood measures is needed as well as long term statistical analysis on more than the three selected events.

In general the proposed combination of nowcast model and stochastic model shows a great potential in rainfall nowcasting with uncertainty estimates and is therefore a promising part of climate solutions in urban areas.

Acknowledgment

The authors would like to thank the Danish Meteorological Institute (DMI) free delivery of radar data. The work is part of the Storm and Wastewater Informatics (SWI) project partly financed by the Danish Agency for Science, Technology, and Innovation.

References

Achleitner, S., Fach, S., Einfalt, T., Rauch, W., 2009: Nowcasting of rainfall and of combined sewage flow in urban drainage systems, *Water Science and Technology* Volume 59, Issue 6.

Aspegren H., Bailly C., Mpe A., Bazzurro N., Morgavi A., Prem E., Jensen N.E., 2001: Radar based rainfall forecast for sewage systems control, *Water Science and Technology*, Volume 43, Issue 5.

Beven, K. J. and Binley, A., 1992: The Future of Distributed Models - Model Calibration and Uncertainty Prediction. *Hydrological processes* 6 (3), 279-298.

Beven, K. J., 2006: A manifesto for the equifinality thesis. *Journal of Hydrology* 320 (1-2)

Borga, M., 2002: Accuracy of radar rainfall estimates for streamflow simulation, *Journal of Hydrology*, vol. 267, no. 1-2,

Einfalt, T., Arnbjerg-Nielsen, K., Golz, C., Jensen, N.E., Quirmbach, M., Vaes, G., Vieux, B., 2004: Towards a roadmap for use of radar rainfall data in urban drainage, *Journal of Hydrology*, vol. 299, no. 3-4.

Fabry, F., Seed, A.W., 2009: Quantifying and predicting the accuracy of radar-based quantitative precipitation forecasts *Advances in Water Resources* 32 (7), pp. 1043-1049

Gill, R. S., Overgaard, S., Bøvith, T., 2006: The Danish weather radar network, *Proceedings of Fourth European Conference on Radar in Meteorology and Hydrology 2006*.

Grecu, M., Krajewski, W.F., 2000, Simulation study of the effects of model uncertainty in variational assimilation of radar data on rainfall forecasting Journal of Hydrology 239 (1-4), pp. 85-96

Li, L., Schmid, W., Joss, J., 1995: Nowcasting of motion and growth of precipitation with radar over a complex orography. *Journal of Applied Meteorology*. 34, 1286– 1300.

Marshall, J.S., and W.M. Palmer, 1948: The distributions of raindrops with size. *Journal of Meteorology*, Vol. 5.

Mecklenburg S, Joss J, Schmid W., 2000: Improving the nowcasting of precipitation in an Alpine region with an enhanced radar echo tracking algorithm. *Journal of Hydrology* 239: 46–68.

Rinehart, R.E., Garvey, E.T., 1978: Three-dimensional storm motion detection by conventional weather radar. *Nature* 273, 287– 289.

Schellart, A.N.A. Rico-Ramirez, M.A., Liguori, S., Saul, A.J., 2009, Quantitative precipitation forecasting for a small urban area: use of radar nowcasting. *Proceedings of the 8th International workshop on precipitation in urban areas, 10-13 December, 2009, St. Moritz, Switzerland*

Thorndahl, S., Beven, K.J., Jensen, J.B., Schaarup-Jensen, K, 2008: Event based uncertainty assessment in urban drainage modelling, applying the GLUE methodology. *Journal of Hydrology*, 357 (3-4), pp. 421-437.

Thorndahl, S., Rasmussen, M.R., Grum, M., Neve, S.L.,2009: Radar based flow and water level forecasting in sewer systems – a Danish case study, *Proceedings of the 8th International workshop on precipitation in urban areas, 10-13 December, 2009, St. Moritz, Switzerland.*

Thorndahl, S., Rasmussen, M.R., 2009: Calibration of a marine X-band radar for precipitation measurements, *Proceedings of the 8th International workshop on precipitation in urban areas, 10-13 December, 2009, St. Moritz, Switzerland.*

Thorndahl, S., Rasmussen, M.R., Neve, S., Poulsen, T.S., Grum, M., 2010: Vejrradarbaseret styring af spildevandsanlæg, Projektrapport, Aalborg Universitet og Krüger ISSN 1901-726x (*in Danish*)

Van Horne, M.P.,2002: Short-term precipitation nowcasting for composite radar rainfall fields. Master's thesis, Massachusetts Institute of Technology.

Villarini, G., Krajewski, W.F., 2010: Review of the different sources of uncertainty in single polarization radar-based estimates of rainfall. *Surveys in Geophysics*, 31 (1), pp. 107-12

Villarini, G., Serinaldi, F., Krajewski, W.F, 2008: Modeling radar-rainfall estimation uncertainties using parametric and non-parametric approaches. *Advances in Water Resources*, 31 (12), pp. 1674-1686.